Functional imaging of biological tissues based on diffuse reflectance spectroscopy with a digital RGB camera

Izumi Nishidate
Graduate School of Bio-Applications & Systems Engineering, Tokyo University of Agriculture and Technology,
2-24-16 Naka-cho, Koganei, Tokyo 184-8588 Japan
E-mail:inishi@cc.tuat.ac.jp

Abstract We investigated a method to quantify the concentrations of chromophores in biological tissue from digital RGB images that is specifically developed for functional imaging of biological tissue. *In vivo* experiments with the human skin tissue during normal and occluded conditions demonstrated the ability of the method to evaluate physiological functions of tissues.

Keywords: diffuse reflectance spectroscopy, Monte Carlo simulation, hemoglobin, optical properties

1. Introduction

Quantitative assessment of biological chromophores (i.e., oxygenated hemoglobin, deoxygenated hemoglobin, and melanin), is important for monitoring tissue metabolism and health status, evaluating tissue viability in surgery and convalescence, and clinical and physiological assessments of vascular functions. The diffuse reflectance spectrum of a living tissue reflects the optical absorption spectra of chromophores, and these spectra depend on the concentrations of chromophores in the tissues. Diffuse reflectance spectroscopy (DRS) has been widely used for the evaluation of chromophores in living tissue [1,2]. The multispectral imaging technique is a useful tool for extending DRS to the spatial mapping of the chromophores in the tissues. This can be simply achieved by a monochromatic charge-coupled device (CCD) camera with narrowband filters and a white light source, which has been used to investigate the hemoglobin perfusion in living tissue [3,4]. In clinical conditions, simpler, more cost-effective and more portable equipment is needed. The digital red, green, blue (RGB) imaging is a promising tool for satisfying these demands for practical application. Imaging with broadband filters, as in the case of digital RGB imaging, can also provide spectral images without mechanical rotation of a filter wheel [5,6]. In this paper, a simple imaging technique [7] using a digital RGB camera are applied to *in vivo* functional imaging of human skin tissues.

2. Principle

RGB-values of a pixel on a skin surface image acquired by a digital camera can be expressed as $[R, G, B]^{\mathrm{T}}=\mathbf{L_1}\times[X, Y, Z]^{\mathrm{T}}$, where $[]^{\mathrm{T}}$ represents transposition of a vector. and X, Y, and Z are the tristimulus values in the CIEXYZ color system and are defined as $X=\int E(\lambda)\bar{x}(\lambda)O(\lambda)d\lambda$, $Y=\int E(\lambda)\bar{y}(\lambda)O(\lambda)d\lambda$, and $Z=\int E(\lambda)\bar{z}(\lambda)O(\lambda)d\lambda$. $\mathbf{L_1}$ is a transformation matrix to convert *XYZ*-values to the corresponding *RGB*-values and it is available for each working space. λ, $E(\lambda)$, and $O(\lambda)$ are wavelength, spectral distribution of illuminant, and the diffuse reflectance spectrum of living tissue, respectively. $\bar{x}(\lambda)$, $\bar{y}(\lambda)$, and $\bar{z}(\lambda)$ are color matching functions in the CIEXYZ color system. Integrals are executed over the visible wavelength range (400 to 700 nm). Assuming that the skin tissue consists of epidermis containing the melanin and dermis containing oxygenated and deoxygenated blood, the diffuse reflectance of skin tissue O can be expressed as

$$O=\frac{I}{I_0}=\left[\int_0^\infty p_e\left(\mu_{s,e},g_e,l_e\right)\exp\left(-\mu_{a,m}l_e\right)dl_e\right]\times\left[\int_0^\infty p_d\left(\mu_{s,d},g_d,l_d\right)\exp\left(-\left(\mu_{a,ob}+\mu_{a,db}\right)l_d\right)dl_d\right], \quad (1)$$

where, I_0 and I are incident and detected light intensities, respectively. $p(\mu_s, g, l)$ is the path length probability function that depends on the scattering properties as well as on the geometry of the measurements. μ_s, g, C, ε, and l, are the scattering coefficient, anisotropy factor, concentration, extinction coefficient, and photon path length, respectively. Subscripts *e*, *d*, *m*, *ob*, and *db* indicate epidermis, dermis, melanin, oxygenated blood, and deoxygenated blood, respectively. Therefore, the RGB values depend on the chromophore concentrations C_m, C_{ob}, and C_{db}. In the proposed method, *RGB*-values are transformed into *XYZ*-values by a matrix $\mathbf{N_1}$ as $[X, Y, Z]^{\mathrm{T}}=\mathbf{N_1}\times[R, G, B]^{\mathrm{T}}$ in each pixel of the image. We determined the matrix $\mathbf{N_1}$ based on measurements of Macbeth Color Checker standard which has 24 color chips and it is supplied with data giving the CIEXYZ values for each chip under the specific illumination and corresponding reflectance spectra. The values of X, Y, and Z are then transformed into C_m, C_{ob}, and C_{db} by a matrix $\mathbf{N_2}$. We calculated 300 diffuse reflectance spectra $O(\lambda)$ in a wavelength range from 400 to 700 nm at intervals of 10 nm by the MCS for light transport [8] in skin tissue under various values of C_m, C_{ob}, and C_{db} and, then, obtained the corresponding X, Y, and Z. The multiple regression analysis with 300 data sets established the three regression equations for C_m, C_{ob}, and C_{db} as $C_m=a_0+a_1X+a_2Y+a_3Z$, $C_{ob}=b_0+b_1X+b_2Y+b_3Z$, and $C_{db}=c_0+c_1X+c_2Y+c_3Z$. The regression coefficients a_i, b_i, and c_i (i=0, 1, 2, 3) reflect the contributions of the *XYZ*-values to C_m, C_{ob}, and C_{db}, respectively, and were used as the elements of a four-by-three matrix $\mathbf{N_2}$. Transformation with $\mathbf{N_2}$ from the tristimulus values to the chromophore concentrations is thus expressed as $[C_m, C_{ob}, C_{db}]^{\mathrm{T}}=\mathbf{N_2}[1, X, Y, Z]^{\mathrm{T}}$. Once we determine the matrices $\mathbf{N_1}$ and $\mathbf{N_2}$, images of C_m, C_{ob}, and C_{db} are reconstructed without the MCS. Total blood concentration image is simply calculated as $C_{tb}=C_{ob}+C_{db}$. Tissue oxygen saturation image can also be reconstructed as $StO_2=(C_{ob}/C_{tb})\times100$.

3. Experimental results and discussion

A metal halide lamplight illuminated the surface of a sample via a light guide with a ring illuminator. Diffusely reflected light was captured by a 24-bit RGB CCD camera and a camera lens to acquire an RGB color image. A standard white diffuser with 99% reflectance was used to correct for the inter-instrument differences in the output of the camera and the spatial non-uniformity of the illumination. Figure 1 shows the typical images of C_{tb}, StO_2 and Cm during cuff occlusion at pressure of 250 mmHg . During the cuff occlusion, StO_2 falls gradually whereas C_{tb} increases slightly. After the cuff was deflated, both StO_2 and C_{tb} increased sharply and, then, gradually returned to their normal levels. In spite of the remarkable changes in StO_2 and C_{tb}, C_m which is independent of temporary hemodynamics remains almost unchanged during the measurement. The method was next applied to *in vivo* noncontact plethysmographic imaging. In this case, the RGB images of 6 subjects were recorded at 15 frames per second (fps). Figure 2 shows the results obtained from a human hand for (a) RGB images, (b) C_{tb} images, (c) comparison between a raw signal of C_{tb} averaged over the region of interest on a fingertip and the filtered signals by the fast Fourier transform (FFT) band pass filter (0.75-2.9Hz) and (d) the plethysmograpic images reconstructed from the alternating current (AC) component of filtered signal in each pixel of C_{tb} images. In Fig.2(c), high frequency fluctuation due to noise in CCD sensor and low frequency component originated from vasomotor are observed in raw signal of C_{tb}. The well-known cardiac pulse wave with two peaks can be observed periodically in the filtered signal. Pulsation of blood volume and its spatial distribution were successfully obtained by the proposed method in Fig.2 (d) whereas both of RGB and C_{tb} images appear to be constant in Figs.2 (a) and 2(b). Average heart rates were estimated from the filtered signal to be 73 ± 9 [bpm], which corresponds to the values of 72 ± 7 [bpm] measured by the commercially available digital pulse monitor.

4. Conclusion

We demonstrated an imaging technique with a digital RGB camera for *in vivo* functional imaging of human skin tissue. The experimental results indicated the ability to evaluate the physiological reactions and hemodynamics in the biological tissues. The great advantages of this method are its simplicity and applicability, because the only devices required are a digital RGB camera with a known color profile, a white light source, and a personal computer.

References

[1] G. N. Stamatas and N. Kollias, "Blood stasis contributions to the perception of skin Pigmentation," J. Biomed. Opt. **9**, 315-322 (2004).

[2] I. Nishidate, Y. Aizu, and H. Mishina, "Estimation of melanin and hemoglobin in skin tissue using multiple regression analysis aided by Monte Carlo simulation," J. Biomed. Opt. **9**, 700-710 (2004).

[3] A. K. Dunn, A. Devor, H. Bolay, M. L. Andermann, M. A. Moskowitz, A. M. Dale, and D. A. Boas, "Simultaneous imaging of total cerebral hemoglobin concentration, oxygenation, and blood flow during functional activation," Opt. Lett. **28**, 28-30 (2003).

[4] A. Basiri, M. Nabili, S. Mathews, A. Libin, S. Groah, H. J. Noordmans, and J. C. Ramella-Roman, "Use of a multi-spectral camera in the characterization of skin wounds," Opt. Express **18**, 3244-3257 (2010).

[5] N. Tsumura, H. Haneishi, and Y. Miyake, "Independent-component analysis of skin color image," J. Opt. Soc. Am. **A16**, 2169–2176 (1999).

[6] S. Chen and Q. Liu, "Modified Wiener estimation of diffuse reflectance spectra from RGB values by the synthesis of new color for tissue measurements," J. Biomed. Opt. **17**, 030501 (2012).

[7] I. Nishidate, N. Tanaka, T. Kawase. T. Maeda, T. Yuasa, Y. Aizu, T. Yuasa, and K. Niizeki, "Noninvasive imaging of human skin hemodynamics using a digital red-green-blue camera," J. Biomed. Opt. **16**, 086012 (2011).

[8] L.-H. Wang, S. L. Jacques, and L.-Q. Zheng, "MCML-Monte Carlo modeling of photon transport in multi-layered tissues," Comput. Methods Programs Biomed. **47**, 131-146 (1995).

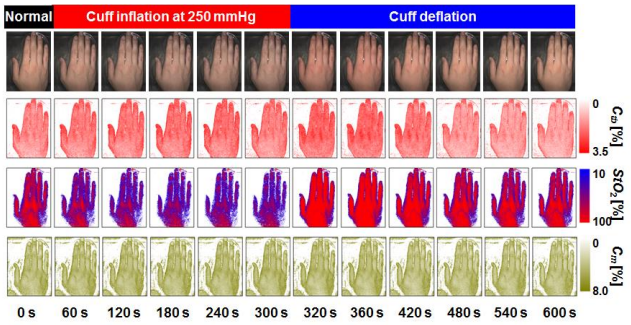

Fig. 1 Typical images obtained from a human hand during cuff occlusion at pressure of 250 mmHg (from top to bottom: RGB image, C_{tb}, StO_2 and Cm).

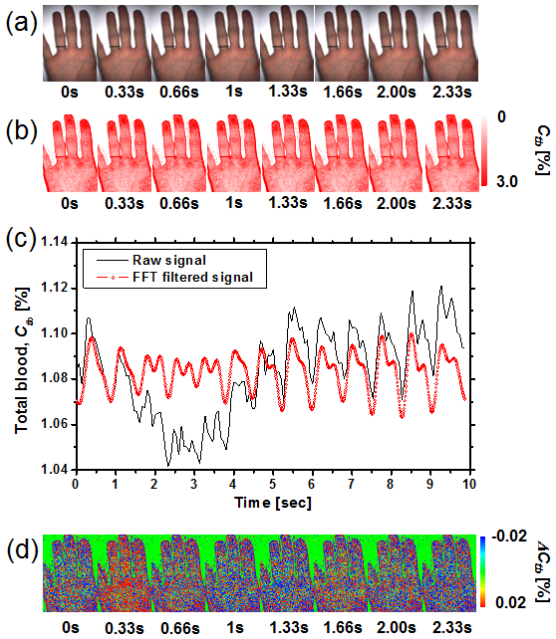

Fig. 2 Typical results obtained from a human hand for (a) RGB images, (b) C_{tb} images, (c) the comparison between the raw signal of C_{tb} averaged over the region of interest on a fingertip and the filtered signals by the FFT band pass filter (0.75-2.9Hz) and (d) the plethysmograpic images reconstructed from the filtered signal in each pixel of C_{tb} images.